Journal of Molecular Liquids 345 (2022) 117450

Contents lists available at ScienceDirect

Journal of Molecular Liquids

journal homepage: www.elsevier.com/locate/molliq

Bioadhesive liquid crystal systems for octyl methoxycinnamate skin delivery

Alice Haddad do Prado [a,1], Jonatas Lobato Duarte [a,1], Leonardo Delello Di Filippo [a], Francesca Damiani Victorelli [a], Marcia Carvalho de Abreu Fantini [b], Rosângela Gonaçalves Peccinini [a], Marlus Chorilli [a,*]

[a] School of Pharmaceutical Sciences, Department of Drugs and Medicines, São Paulo State University (UNESP), Rodovia Araraquara-Jaú, km. 1. Araraquara, São Paulo 14801-902, Brazil
[b] Institute of Physics – São Paulo University – São Paulo, SP 05315-970, Brazil

ARTICLE INFO

Article history:
Received 24 March 2021
Revised 27 August 2021
Accepted 31 August 2021
Available online 3 September 2021

Keywords:
Nanotechnology
Surfactant systems
Sunscreen filter
Skin permeation

ABSTRACT

Excessive exposure to ultraviolet radiation stemmed from sunlight can cause harm to human skin. An alternative to avoid and reduce the effects of ultraviolet radiation is the use of sunscreens. The sunscreen octyl methoxycinnamate (OMC) is one of the most used filters globally. Still, studies have indicated systemic absorption of this product and subsequent amendment and impaired functioning of the endocrine system. Surfactant systems as liquid crystals systems are used to improve the delivery and efficacy of active ingredients. The OMC incorporated into liquid crystals can have greater retention in the skin's outer layers and lower percutaneous absorption, avoiding their harmful systemic effects. This work aimed to develop and characterize surfactant-based systems for OMC skin delivery and evaluate the *in vitro* skin permeation and retention properties. Polarized light microscopy and SAXS showed that the selected formulations presented cubic mesophases. The formulations presented pseudoplastic behaviour and the F1 and F1F formulations presented the highest viscosity of all formulations. The three formulations presented controlled release over time, being the F2F and F3F presenting high release rates when compared to F1F. The formulation F3F presented the higher stratum corneum retention and lower epidermis and dermis retention when compared to F1F and F2F. The formultions manteined the sun protecting factor of OMC, being similar to the finds in the literature for this sunscreen. Thus, the bioadhesive LCS developed in this work have great potential for OMC delivery to the skin.

1. Introduction

Excessive exposure of human skin to ultraviolet (UV) radiation is a well-known risk factor for developing burns and skin cancer [1]. Besides, it can cause rashes, eye diseases, DNA damage, premature aging of the skin, and immunosuppression [2,3]. To protect the skin, sunscreens absorb UV radiation in a broad spectrum, physically cover and adhere well to the skin, and resist water removal. Also, it should remain in the outer layer of the skin with minimal permeation into the systemic circulation [4].

The octyl methoxycinnamate (OMC) is an organic UVB sunscreen derived from cinnamic acid and developed in the 1950 s. It is a transparent, oily, slightly yellow, and odorless liquid used in various cosmetic products. Because of their poor water solubility characteristic, it is primarily included in products that require water resistance. In Brazil, Japan, and Europe, its maximum allowed concentration is 10%, and the United States is 7.5% [4–6].

Some studies have shown the systemic distribution of OMC, which can be found in blood, urine, and milk samples after systemic and topical application, indicating systemic exposure and possible endocrine disruption [7–11], is necessary the development of sunscreen formulations with low skin permeation.

It is known that the performance of a sunscreen formulation depends not only on the intrinsic properties of the filters but the vehicle used. Thus, to increase the retention of sunscreen on the skin, studies involving more suitable carriers to incorporate filters have been performed. Some studies showed that OMC in delivery systems has increased skin retention, decreases skin penetration, reduced photobleaching, and increased photoprotection [4,12–14]. These features have attracted significant attention because of topical delivery advantages [1].

* Corresponding author.
E-mail address: marlus.chorilli@unesp.br (M. Chorilli).
[1] These authors contributed equally to this work.

https://doi.org/10.1016/j.molliq.2021.117450
0167-7322/

Among these systems, liquid crystalline systems (LCSs) and microemulsions (MEs) for topical drug delivery can be used. The surfactant in these systems could stabilize components with different polarities and characteristics, being versatile systems [15–17].

The liquid crystalline systems (LCSs) have mechanical properties similar to liquids, featuring their fluidity and optical, electrical, and magnetic properties similar to the solids, which characterize their structure, orientation, and/or position. Therefore represent an intermediate state between solid and liquid, called mesophases, and is formed spontaneously in the oil and water interface [18–23]. Together these characteristics make these systems candidates with the potential to improve the topical performance of sunscreens such as the OMC.

They are divided into two classes: Thermotropic, where the temperature is the essential parameter; and lyotropic, formed after the addition of a solvent [19,24–27]. Certain surfactants may provide lyotropic liquid crystals in the water at a given temperature and concentration. As the surfactant concentration increases, it can be obtained in different SLC ways: lamellar, hexagonal, and cubic [28].

The LCSs have applications that meet current expectations for topical use [29,30]. Its use in cosmetics has the advantages of increased stability and solubility, incorporation and controlled delivery of active, since the liquid crystal protect sensitive active substances against thermal degradation and photodegradation and promote increased water retention in the stratum corneum, providing more skin hydration [19,29,31,32]. In this way, this study aimed to develop an OMC-loaded liquid crystal system for skin delivery.

2. Materials and methods

2.1. Materials

PPG-5-CETETH-20 - Procetyl AWS® (Croda, Brazil); Polycarbophil – NOVEON® AA-1 (Lubrizol, USA), Silicone glycol copolymer - DC® 193 (Dow Corning®, USA), Octyl methoxycinnamate – (Deg - Brazil). Triethanolamine (Deg- Brazil). Purified water (Millipore Milli-Q® Plus, Germany).

2.2. Ternary phase diagram (TFD)

TFD was constructed point by point by mixing different proportions of silicone glycol copolymer - DC® 193, PPG-5-CETETH-20, a dispersion of Noveon® AA-1 (polycarbophil) 0.5%, at room temperature (25 ± 0.5C). Noveon® AA-1 dispersion had his pH adjusted to 7.0 with the aid of triethanolamine (Deg, Brazil). The obtained formulations were characterized visually and by polarized light microscopy.

3. Physical-chemical characterization of the selected formulations

3.1. Polarized light microscopy (PLM)

The samples were analyzed in a polarized light microscope (Olympus BX41) coupled with a QColor3 camera (Olympus America Inc) under a magnification of 20x at room temperature (25 ± 0.5 °C).

3.2. Small-angle X-ray scattering (SAXS)

The selected formulations were characterized by small-angle X-ray scattering (SAXS) performed on a Xeuss 1.0 (Xenocs) instrument equipped with a microfocus Genix 3D system (Xenocs) and a Pilatus detector (Dectris). The sample-to-detector distance was ~ 667 mm, which provided an effective range of the modulus of the transfer moment vector, $q = [4\pi \sin(\theta)]/\lambda$ (where 2θ is the scattering angle and λ = 1.5418 Å is the X-ray wavelength), experimentally accessible from 0.01 to 0.47 $Å^{-1}$. The samples were filled into reusable quartz capillaries with 1.5 mm in diameter mounted on stainless steel cases. All measurements were performed at room temperature, RT = (22 ± 1) °C, and the data treatment, which includes azimuthal integration, background subtraction, and absolute scale normalization, was performed using phyton programs developed by Complex Fluids Group of Institute of Physics -- São Paulo University.

3.3. Rheological analysis

For rheological analyses, a controlled-stress AR 2000 Rheometer (TA Instruments, New Castle, DE, USA) with cone-plate geometry (diameter – 40 mm, 2-degree angle, gap – 52 um). The tests were performed in triplicate at a temperature of 32 ± 0.5 °C, and the study was conducted by Software Data Analysis.

3.3.1. Determination of flow properties

For this analysis, a small quantity of formulation was placed on the rheometer's bottom plate. The shear rate was 0–100 s^{-1} for the ascending and 100–0 s^{-1} for the descending curve with 120 s in each curve. Data points of ascending curves were fitted by Power Law's model using Eq. (1)

$$\tau = k\gamma^n \quad (1)$$

Where τ - shear rate, k consistency index, γ - shear stress, and n – flow behavior.

3.3.2. Oscillatory analyses

The stress sweep was carried out at a constant frequency (0.6283 rad/s) over the stress range of 0–50 Pa. After determining the tension of 1 Pa viscoelastic region, the rheometer was put in the frequency sweep mode for performing the frequency scan test, in order to determine the storage modulus G' and G". The frequency range from 0.6283 to 62.831 rad/sec and a pressure of 1 Pa were used for this test.

3.4. Texture profile analysis

The texture profile of selected systems was obtained in a texture analyzer TAXT plus (Stable Micro Systems, England). 7.5 g of the formulations were centrifuged (717 RCF, 10 min) to remove air bubbles and smooth the formulation surface, stored 24 h before the test. Then, the sample tubes were placed under the texture analyzer probe (10 mm diameter), programmed to compress the sample at a speed of 0.5 mm/s until a pre-set depth of 10 mm and return to the sample's surface at the same speed. After 5 s of rest, the program is repeated. The analyses were performed in triplicate at 32 ± 0.5° C.

3.5. In vitro evaluation of the bioadhesive force

A texture analyzer TAXT plus (Stable Micro Systems, England) was used for this experiment. The pig ear skin used was dermatomised as described in the In Vitro Skin Permeation and Retention Studies (section 3.6). The pig ear skin was attached to the analytical probe and fixed with a rubber ring. The probe was lowering at a constant speed (1 $mm{\cdot}s^{-1}$) until the contact with the formulations and kept in contact for 60 s and raised in 0.5 $mm{\cdot}s^{-1}$. With the results obtained, a force curve versus distance was built, where they have obtained values of the separation force, the

contact time, the peak of force, traction, and work the system deformation until rupture. Assays were performed in triplicate.

3.6. In vitro skin permeation and retention studies

Pig ear obtained from a local slaughterhouse was used in this experiment. The ears were cleaned in freshwater, the excess hair was removed with scissors, and the stratum (SC) corneum and epidermis + dermis (ED) were isolated with a dermatometer (Nouvag TCM 300, Goldach, Switzerland) [33]. The *in vitro* permeation test was conducted using a vertical diffusion cell system (Franz cell). The medium receptor volume is 7.0 mL, and the area available for diffusion was 1.77 cm^2. The receptor solution consisted of pH 7.4 phosphate buffer with polysorbate 80 2.0% (w/v), ensuring sink conditions throughout the test. The samples were weighed (400 mg) and transferred to the injector ring placed on pig ear skin. The experiments were conducted at 32 ± 2 °C, and the receptor solution was continuously stirred at 300 rpm. During the test, 2 mL aliquots were collected at 1, 2, 4, 6, 8, 10, and 12 h, filtered through a membrane of 0.45 pore size and analyzed by ultra-high performance liquid chromatography (UPLC) [34] to evaluate the permeation of the OMC. After permeation, the skins were removed from the equipment and placed on a glass plate to hold skin retention. The first step was to hold the tape stripping technique. The SC was removed by consecutive adhesive tape (3 M Scotch 720®) [35]. First, this excess formulation was removed from the skin with absorbent paper, and the stratum corneum was removed by using 15 tapes. The tapes were placed in test tubes containing 3 mL of isopropanol solvent extractor, vortexed for 2 min, and sonicated for 30 min in an ultrasonic bath (at room temperature). The supernatant was filtered and analyzed by UPLC to quantify the OMC retained in the stratum corneum. After removing the SC, the area in contact with the formulation was cut using surgical scissors. The skin was transferred to test tubes containing 3 mL of isopropanol. The same procedure described above was performed, but this time, after stirring for 2 min, the solution was triturated for 1 min with high energy homogeinazation (Ultra-Turrax® - IKA), sonicated for 30 min, and centrifuged for 7 min at 3000 rpm. The supernatant was filtered and analyzed by UPLC to quantify the OMC retained in the epidermis + dermis. This secondary test was properly called dermal retention in this work. The data obtained were statiscally analysed by ANOVA test in Graphpad Prism 9 software.

3.7. In vitro sun protection factor (SPF)

The SPF was determined by the absorption spectra of the formulations in ethanol [36]. The samples were diluted to a final concentration of 0.2 mg/mL of OMC, and the studies were conducted in the range of 290–320 nm, every 5 nm, and 3 determinations were made at each point. Mansur equation (Eq. (2)) was applied for SPF calculations [37]

$$SPF = CF \times \sum_{290}^{320} [E(\lambda) \times I(\lambda) \times A(\lambda)] \quad (2)$$

Where CF is the correction factor of 10; E(λ) is the erythema effect of radiation at wavelength (λ); I(λ) is the sunlight intensity at wavelength (λ); Abs(λ) is the absorbance value of the solution at a wavelength (λ). The E(λ) and I(λ) are constants determined by Sayre et al [38]. The data obtained were statistically analyzed by ANOVA test in Graphpad Prism 9 software.

4. Results and discussion

4.1. Ternary phase diagram construction and preparation of LCSs

The ternary phase diagram is represented by an equilateral triangle where its sides are equivalent to the oil phase (O), aqueous (A), and surfactant (S). Varying these three components' concentration is possible to obtain a wide variety of formulations differing in their physical–chemical behavior. Therefore, the ternary diagram's construction is an excellent design tool that provides an overview indicating where liquid–crystal phase transitions occur [39]. The ternary diagram obtained was characterized visually according to the fluidity and translucency of the systems and classified as transparent viscous system (TVS), translucent viscous system (TrVS), transparent liquid system (TLS), and translucent liquid system (TrLS). This classification resulted in the diagram shown in Fig. 1. The increase in water concentration (up to 40%) leads to the transition of TLS to TrVS, similar to the results observed by our previous work [40], which can be related to the increase in the amount of polycarbophil, dispersed in the aqueous phase. When the aqueous phase is increased above 60%, and the concentration of surfactant is below 30% TVS are obtained. The increase in the water content can change the surfactant curvature, which can change the LCS mesophases. Additionally, other reports indicate that surfactants concentration ranging from 30 to 40% generates translucent viscous systems similar to previous works of our group, which can indicate the obtention of LCS in this surfactants ratio [40,41]. The self-assembly characteristic of LCS can be explained by the critical packing parameter of the surfactants and depends on the concentration and shape of the surfactant used [42,43]. The increase in water content led to more viscous and organized formation, which can be critical to LCS development in drug delivery [44]. Additionally, the ingredients used in these formulations show higher biocompatibility and no toxicity [20,45,46].

4.2. Physical-chemical characterization of selected formulations

4.2.1. Polarized light microscopy (PLM)

Most systems presented a dark field, with one point (27) showing striated structures, similar behavior found by Chorilli et al. [26]. Isotropic systems with a dark field in PLM are characteristics of liquid crystalline cubic phase systems [47], which cannot deflect the plane of polarized light. The points 22, 23, and 24 were renamed as F1, F2, and F3 and selected to the following stages of this study based on the visual characteristics and by previous results of our group that showed that similar formulations presented excellent properties as carriers for topical delivery of actives ingredients [33,40,41,48]. After adding the OMC in the F1, F2, and F3 the dark field characteristic did not change (Fig. 2-B) but visually, the formulations presented as more opaque systems, as seen in Fig. 2-A. The composition of each system used is showed in Table 1.

4.2.2. SAXS xxx

The cubic mesophase was confirmed by the SAXS analysis, as can be seen in Fig. 3. Also, the introduction of OMC did not lead to mesophase changing. Similar results were found by Brinon et al. that when adding OMC in a Water–C12EO23–C12EO4 system, the cubic mesophases did not present phase transition [13]. This type of mesophase can be explored as a drug delivery system, controlling the release of active ingredients from its structures [49] and can be applied in the skin diminishing the transcutaneous fluxes when compared to other mesophases, as lamellar liquid crystals [13].

There is an increase in the lattice parameter with the introduction of the OMC. $d = 2\pi/q$ (d is inter-planar distance, which is

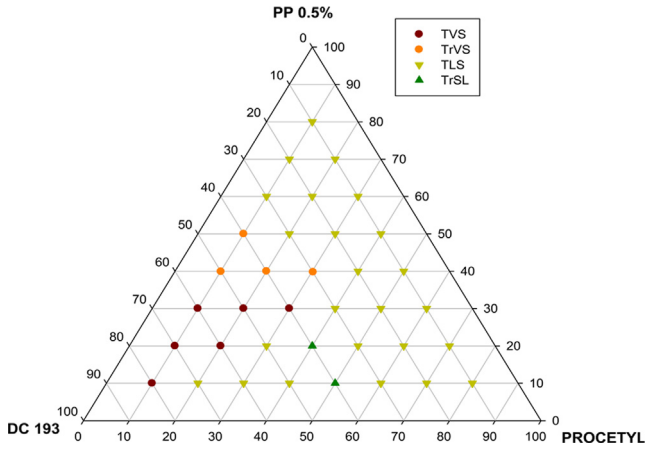

Fig. 1. Ternary phase diagram composed of PPG-5- CETETH-20 (Procetyl AWS®), silicone glycol copolymer - DC® 193 (DC 193), and an aqueous dispersion of Noveon® AA-1 (polycarbophil) 0.5% (PP 0.5%).

proportional to lattice parameter). Which means, if q decreases, d increases. The wider are the peaks, the larger is the structural disorder. Also, it is suggested from the spacing ratios that cubic phases of phase D and P can be observed in the formulations [50,51].

4.2.3. Rheological studies

4.2.3.1. Determination of flow properties. The flow rheograms of the formulations are shown in Fig. 4. F1, F3, and F3F showed similar rheological behavior, with linear relationships between the shear stress and shear rate values exhibiting Newtonian flow behavior. F1F, F2, and F2F, it is possible to notice a non-newtonian behavior since there is no linear relation between shear stress and shear rate values [52]. The n-values obtained using Eq. (1) showed that formulations exhibited pseudoplastic behavior, as the obtained n-values were<1 as can be observed in Table 1. This behavior can be explained by the complex internal structure and the intermolecular bonds that are weakened after a shear rate leading to a disorganization of these cubic systems [41,53,54]. The viscosity of formulation F1 increased after the incorporation of OMC and in the formulations F2 and F3 the OMC decreased the viscosity as can be observed in the Table 2 from the consistency index (k).

Pseudoplasticity is a convenient property for topical formulations because it confers to the formulations better flow after tension is applied, leading to uniform distribution of the formulations on the skin. This is due to the polymer chains' deinterlacing and subsequent thinning of the flow that will occur during the product's application to the skin, facilitating its use [39,55]. Formulations F1F, F2, and F2F exhibit thixotropic behavior; this property occurs when the material requires time after applied pressure to recover it's initial internal organization.

4.2.3.2. Oscillatory analyses. The oscillatory analyses of F1, F1F, F2 F2F, F3, F3F are shown in Fig. 5. It is possible to verify that only the F1F shows G'>G", corroborating the results found on the rheological flow analysis. For F2, F2F, F3, and F3F formulation, the G " > G ' demonstrating a more predominant viscous behavior. This difference in the viscoelastic properties can be related to the amount

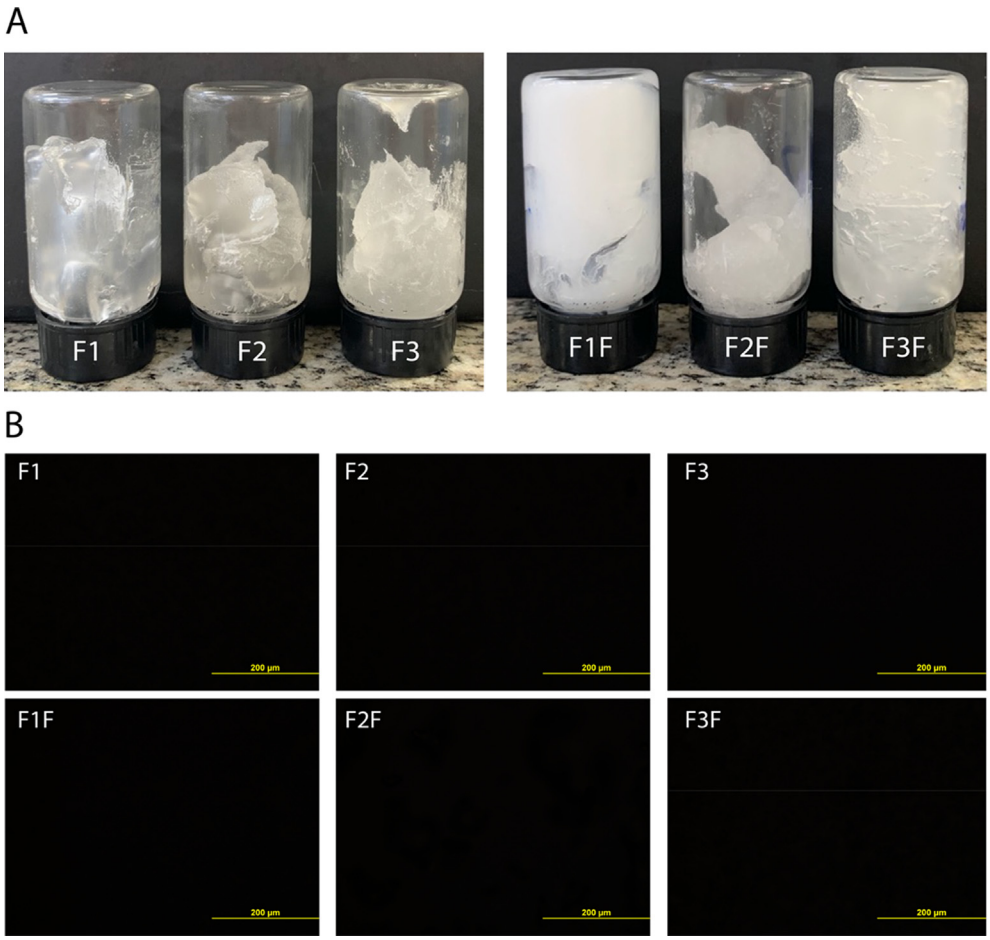

Fig. 2. A – Visual appearance and **B –** Polarized light microscopy exhibiting dark field of formulations F1, F1F, F2, F2F, F3 and F3F. Magnification 20x.

Table 1
Composition of the selected formulations in percentage (%) (w/w).

Formulations	PPG-5-CETETH-20	DC 193	Aqueous phase	OMC
F1	40	10	50	–
F1F	40	10	50	5
F2	40	20	40	–
F2F	40	20	40	5
F3	40	30	30	–
F3F	40	30	30	5

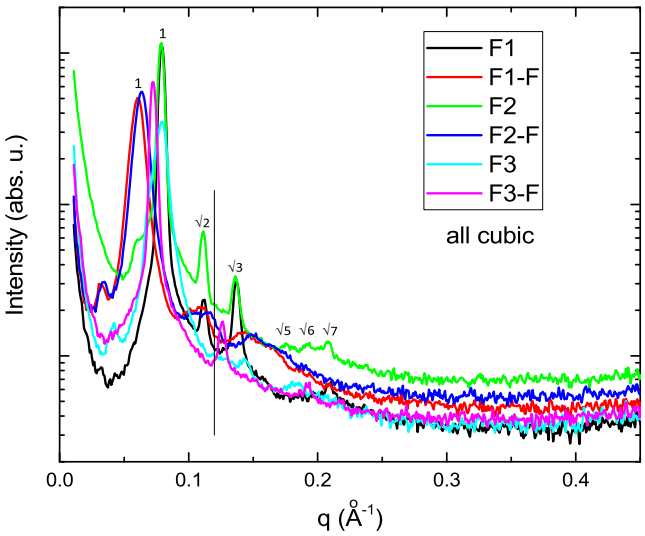

Fig. 3. SAXS results of the F1, F2, F3, F1F, F2F, and F3F formulations.

of the polymer, which in the formulations with more aqueous phase (F1 and F1F), higher amounts of polymer can led to the formation of a more robust internal structure, resulting in the differences in the observed viscoelastic modulus [55]. The elastic behavior is characteristic for cubic mesophases [53,54]

4.3. Texture profile analysis

The texture profile analysis (TPA) reveals the formulation's mechanical characteristics, such as compressibility, hardness, adhesion, and cohesion [22,40,56]. For the formulations F2 and F3, we did not performed the parameters of adhesiveness and cohesiviness probably due to intrinsic characteristics of F2 and F3 formulations, as described by Fonseca-Santos [41]. The parameters collected to F2 and F3 formulations did not show alterations after the adittion of OMC (Table 3).

For formulation F1 and F1F a significat diference in TPA is shown in Table 3 when compared to F2 and F3 formulations. This differences can be explained by the polymer's influence on the viscosity indicating a more organized system, as observed in oscillatory tests on viscoelasticity [55]. Besides, it is suggested that the OMC influenced the systems' structural organization since the rheological tests demonstrated that this sunscreen, under certain con-

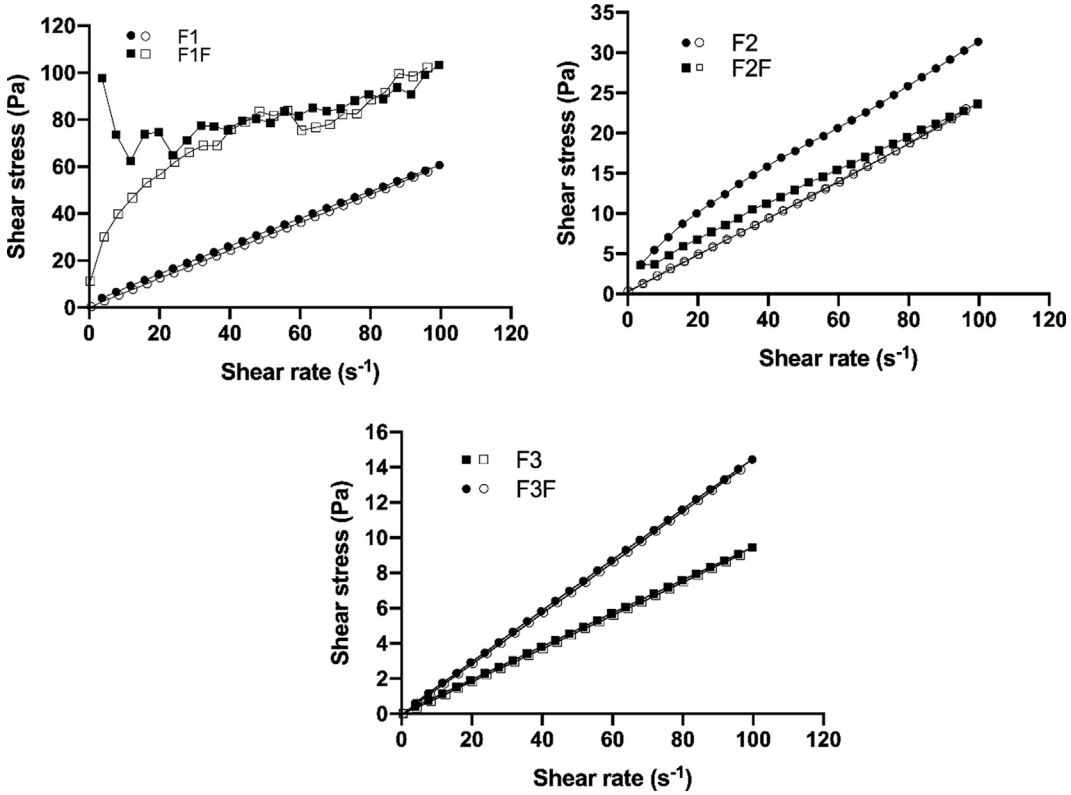

Fig. 4. Flow rheograms of the F1, F2, F3, F1F, F2F, and F3F formulations. Notes: Filled symbols indicate the ascending curves, and open symbols indicate descending curves.

Table 2
Flow behavior (n), consistency index (k) and R values of the LCS

Sample	n	K (Pa.s)	R^2
F1	0.904	0,939	0,999
F1F	0.345	19,9	0,959
F2	0.705	1,18	0,996
F2F	0.766	0,682	0,995
F3	0.987	0,153	0,999
F3F	0.986	0,100	0,999

ditions, can increase the viscosity of the system, as can be observed in the flow reology results in section 4.2.3.1, which may favor the retention of the formulation at the site of application.

4.4. Ex vivo evaluation of the bioadhesive force

Bioadhesion refers to the formulation's ability to attach to biological tissues. Bioadhesive formulations have some advantages over non-bioadhesive ones, as such more excellent retention in the skin, increased contact with the skin, lower application frequency, and better acceptance by the user [39].

The adhesive materials incorporated in pharmaceutical formulations can be hydrophilic molecules of natural or synthetic origin, containing numerous organic functions capable of chemically bonding to the biological surface [55]. Polycarbophil, a negatively charged synthetic polymer derived from polyacrylic acid, has an adhesive behavior due to physical–chemical interactions between the material and the tissue, such as hydrophobic interactions, hydrogen bonds, and van der Waals [58].

Table 4 shows the bioadhesion values for each formulation with and without the sunscreen. From the analysis, it can be seen that the formulation F1, with or without added OMC, presents greater bioadhesive strength (mN) than the others, suggesting the influence of the polymer, which was incorporated in greater quantity for F1 and F1F than the other formulations.

Only the F1F formulation showed a greater difference when compared to the other formulations. In this case, the bioadhesion was relatively high, suggesting that the OMC sunscreen increase the bioadhesion. The rheological properties of liquid-crystalline systems can explain this. The increase in its viscosity and its elastic characteristic contributed to the permanence time increment of the formulation in the intended site of use [39,55]. On the other hand, for the formulations F2, F2F, F3, and F3F, there was no significant increase in the bioadhesive strength. This may be related to lower amounts of polycarbophil, which seems insufficient to promote a synergism capable of increasing the bioadhesion, as observed in the F1 and F1F formulations. Previous works have shown similar behavior [40,41].

4.5. Ex vivo skin permeation and retention

Skin permeation studies are important to optimize dermal and transdermal release formulations [59]. For topical formulations, as the sunscreens, retention in the skin with minimal permeation is desired, whereas, for systemic formulations, the opposite is preferred [35].

In general, the LCS developed presented sustained release over time, as shown in Fig. 6A. This behavior has already been observed in other studies using cubic phase liquid crystals, demonstrating the potential of this type of formulation as a controlled release platform, increasing the retention of active ingredients in the skin and reducing its systemic biodistribution [60]. The formulation with the lowest cumulative release was the formulation F1F. The formulations F2F and F3F were those with the highest cumulative release rates over time. Although there is no statistical significance, it is possible to observe that the F3F formulation presented a more pronounced release rate at the initial times (1, 2, and 4 h). The main reason the F1F formulation has released less OM may be related to the greater amount of polymer in its composition, mak-

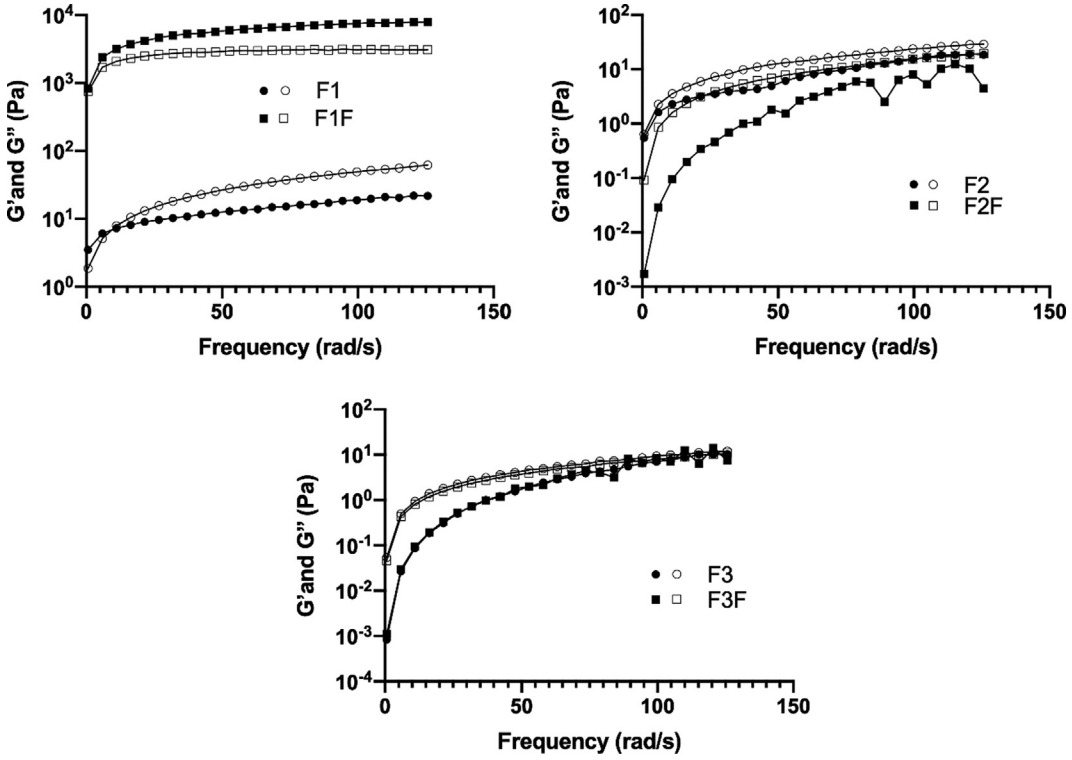

Fig. 5. Frequency sweep profiles of the F1, F1F, F2, F2F, F3, and F3F formulations. Note: Filled symbols indicate the G'modulus, and open symbols indicate the G" modulus.

Table 3
Texture profile analysis of F1 and F1F formulations

	Hardness (N)	Compressibility (N.s)	Adhesiveness (N.s)	Cohesiveness
F1	0.002 ± 0.001	0.085 ± 0.055	0.001 ± 0.000	0.829 ± 0.239
F1F	0.306 ± 0.014	1.972 ± 0.266	0.013 ± 0.000	0.690 ± 0.086
F2	0.002 ± 0.0005	0.070 ± 0.001	*	*
F2F	0.003 ± 0.0005	0.073 ± 0.001	*	*
F3	0.003 ± 0.0005	0.071 ± 0.002	*	*
F3F	0.004 ± 0.0005	0.076 ± 0.002	*	*

*Data not collected.

Table 4
Bioadhesive strength (mN) of the F1, F1F, F2, F2F, F3, F3F formulations.

Samples	(mN)
F1	28.0 ± 2.64
F1F	679.3 ± 95.01
F2	6.33 ± 2.51
F2F	3.67 ± 1.53
F3	4.67 ± 1.15
F3F	4.67 ± 1.15

ing its structure more organized [61,62] and increasing its viscosity, as observed in rheology analyses.

According to the SAXS data, it is suggested that the F3F formulation has the highest degree of organization in its structure when compared to the F1F and F2F formulations because it has narrower peaks, which may also be associated with the trend of higher release rates found for this formulation.

Ideally, sunscreens are impregnated in the stratum corneum, forming a barrier to UV rays without penetrating deeper tissue [63]. As can be seen in Fig. 6 B and C the OMC from the F1F, F2F, F3F showed higher SC than E + D retention values. The F1F formulation showed a lower SC retention value that was a statistically significant compared to the F3F formulation, which can be attributed to its lower cumulative release rates. In addition to presenting good retention, its permeation was minimal, showing the benefits of incorporating the OMC in the LCS. The amount of OMC from the formulations retained in the skin may be related to its lipophilicity, justifying the sunscreen's affinity for the stratum corneum because of the molecular characteristics of OMC, as the polarity of this ingredient (MONTEIRO et al., 2012). The literature shows that the

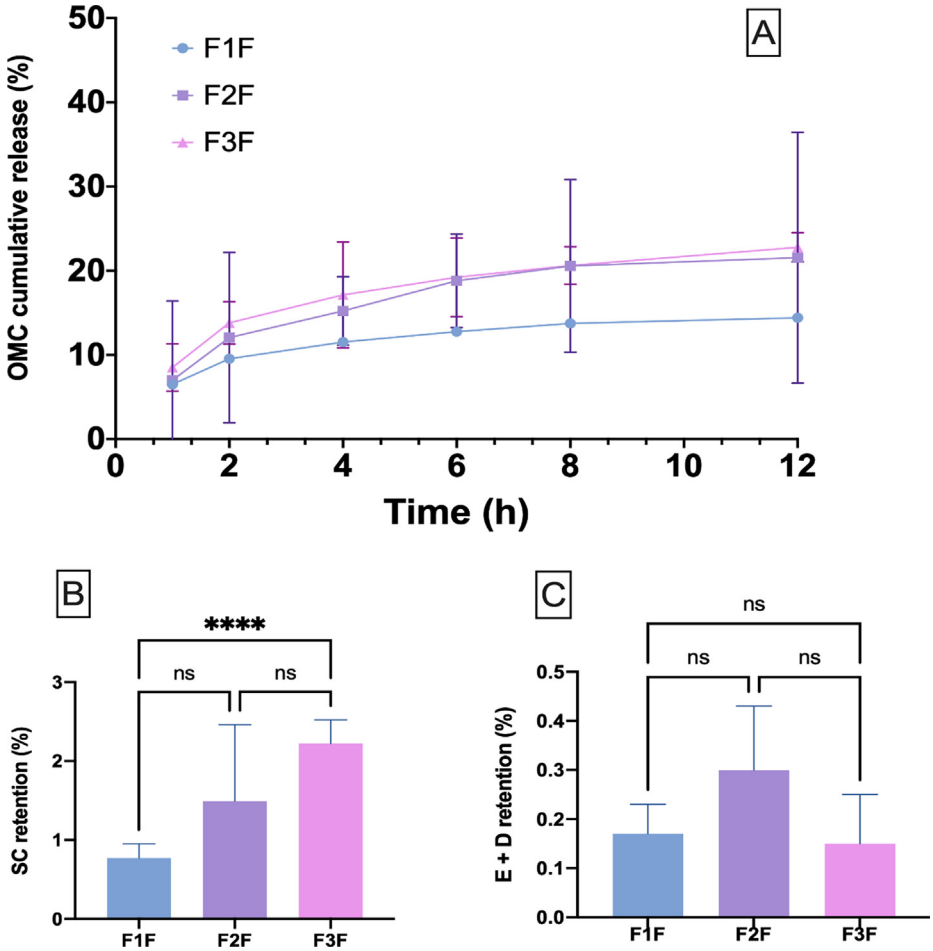

Fig. 6. A Release profile of OMC from F1F, F2F, F3F, B – Stratum corneum retention, and C – Epidermis and dermis retention. (ANOVA **** p-value < 0.0001).

Table 5
In vitro SPF determinations of the formulations containing OMC

Formulations	SPF
Free OMC	44.14 ± 0.20[a]
F1F	37.11 ± 1.71[b]
F2F	37.69 ± 0.44[b]
F3F	37.72 ± 0.25[b]

Same letters in the columns indicate $p < 0.001$ between the means.

use of nanotechnology in the delivery is an excellent strategy to improve the safety of OMC by increase skin retention and decreasing skin permeation [65,66]. Currently, commercially available formulations present a high profile of permeation and systemic biodistribution, representing a health risk for users [67]. The formulations developed in this work demonstrated good skin permeation and retention profiles in the superficial layers of the skin, representing a safer alternative for the use of sunscreens.

4.6. In vitro sun protection factor estimation

In vitro SPF determination tests, such as that previously described by Mansur et al. are important to demonstrate the potential of formulations intended for use as a sunscreen, serving as a tool for screening formulations with photoprotective activity [36].

As can be observed in Table 5 compared to the free OMC, the LCS tested in this study showed a slight decrease in SPF, which may be related to incorporating the OMC in the formulations, which presented sustained release over time. The literature shows similar results to the results obtained in our study[64]. Prado et al. found SPF around 40 in nanostructured lipid carriers with OMC [68]. In other studies, liposomes containing OMC in a concentration of 5.5% (w/w) presented SPF of 13.98 ± 0.66 [69], a value much lower than the finds in our work in a similar amount of OMC (5 % w/w).

5. Conclusion

Motivated by the need to develop an efficient and safe photoprotective formulation for topical use, we develop crystalline liquid systems containing OMC. From the ternary phase diagram, it was possible to obtain cubic mesophase systems, as confirmed by PLM and SAXS analyses. The systems presented rheological properties such as viscosity and elastic properties desirable for for intended site of application.

Ex vivo studies using porcine skin showed that the formulations presented a sustained release profile over time. In addition, the systems presented low cutaneous permeability, as demonstrated by permeation data, where the OMC demonstrated high retention rates in the stratum corneum, a highly desirable characteristic for this type of formulation, since high permeability and systemic absorption are currently a problem, as highlighted in the literature.

The *In vitro* SPF assay demonstrated that after being incorporated into the LCS, OMC maintained its ultraviolet absorption properties, demonstrating the potential of these formulations for the delivery of sunscreens for topical application.

CRediT authorship contribution statement

Alice Haddad Prado: Data curation, Investigation, Visualization, Writing – original draft. **Jonatas Lobato Duarte:** Formal analysis, Writing – original draft, Investigation, Writing – review & editing. **Leonardo Delello Di Filippo:** Data curation, Investigation, Writing– original draft. **Francesca Damiani Victorelli:** . **Marcia Carvalho Abreu Fantini:** Supervision, Writing – review & editing, Resources. **Rosângela Gonaçalves Peccinini:** Supervision, Resources. **Marlus Chorilli:** Project administration, Funding acquisition, Conceptualization, Resources.

Declaration of Competing Interest

The authors declare that they have no known competing financial interests or personal relationships that could have appeared to influence the work reported in this paper.

Acknowledgments

We thank Fundação de Amparo à Pesquisa do Estado de São Paulo (FAPESP- 14/22426-2; 16/24531-3; 17/209992-9; 17/17844-8), Conselho Nacional de Desenvolvimento Científico e Tecnológico (CNPq) and CAPES. We would like to thank the PhD student Alberto Gomes Tavares Junior for the assistance in the *In vitro* SPF determination experiments and to Professor Estela Sasso Cerri for the use of the PLM in her facilities.

References

[1] L. Shi, J. Shan, Y. Ju, P. Aikens, R.K. Prud'homme, Nanoparticles as delivery vehicles for sunscreen agents, Colloids Surfaces A Physicochem. Eng. Asp. 396 (2012) 122–129, https://doi.org/10.1016/j.colsurfa.2011.12.053.
[2] Jutta Kockler, Michael Oelgemöller, Sherryl Robertson, Beverley D. Glass, Photostability of sunscreens, J. Photochem. Photobiol. C Photochem. Rev. 13 (1) (2012) 91–110, https://doi.org/10.1016/j.jphotochemrev.2011.12.001.
[3] Holly V. DeBuys, Stanley B. Levy, John C. Murray, Doren L. Madey, Sheldon R. Pinnell, Modern Approaches To Photoprotection, Dermatol. Clin. 18 (4) (2000) 577–590, https://doi.org/10.1016/S0733-8635(05)70208-4.
[4] M.M. Jiménez, J. Pelletier, M.F. Bobin, M.C. Martini, Influence of encapsulation on the in vitro percutaneous absorption of octyl methoxycinnamate, Int. J. Pharm. 272 (1-2) (2004) 45–55, https://doi.org/10.1016/j.ijpharm.2003.11.029.
[5] A. Chisvert, M.C. Pascual-Martí, A. Salvador, Determination of the UV filters worldwide authorised in sunscreens by high-performance liquid chromatography, J. Chromatogr. A. 921 (2) (2001) 207–215, https://doi.org/10.1016/S0021-9673(01)00866-4.
[6] Amaris N. Geisler, Evan Austin, Julie Nguyen, Iltefat Hamzavi, Jared Jagdeo, Henry W. Lim, Visible Light Part II. Photoprotection against visible and ultraviolet light, J. Am. Acad. Dermatol. 84 (5) (2021) 1233–1244, https://doi.org/10.1016/j.jaad.2020.11.074.
[7] Marta Axelstad, Julie Boberg, Karin Sørig Hougaard, Sofie Christiansen, Pernille Rosenskjold Jacobsen, Karen Riiber Mandrup, Christine Nellemann, Søren Peter Lund, Ulla Hass, Effects of pre- and postnatal exposure to the UV-filter Octyl Methoxycinnamate (OMC) on the reproductive, auditory and neurological development of rat offspring, Toxicol. Appl. Pharmacol. 250 (3) (2011) 278–290, https://doi.org/10.1016/j.taap.2010.10.031.
[8] Nadeem Rezaq Janjua, Brian Mogensen, Anna-Maria Andersson, Jørgen Holm Petersen, Mette Henriksen, Niels E. Skakkebæk, Hans Christian Wulf, Systemic Absorption of the Sunscreens Benzophenone-3, Octyl-Methoxycinnamate, and 3-(4-Methyl-Benzylidene) Camphor After Whole-Body Topical Application and Reproductive Hormone Levels in Humans, J. Invest. Dermatol. 123 (1) (2004) 57–61, https://doi.org/10.1111/j.0022-202X.2004.22725.x.
[9] M. Schlumpf, K. Kypkec, C. Vöktd, M. Birchlerd, S. Durrerb, O. Faassb, C. Ehnesb, M. Fuetschb, C. Gailleab, M. Henselerb, L. Hofkampe, K. Maerkel, S. Reolon, A. Zenker, B. Timms, J.A.F. Tresguerres, W. Lichtensteiger, Endocrine Active UV Filters: Developmental Toxicity and Exposure Through Breast Milk, Chim. Int. J. Chem. 62 (2008) 688, https://doi.org/10.2533/chimia.2008.345.
[10] JF. Nash, Human Safety and Efficacy of Ultraviolet Filters and Sunscreen Products, Dermatol. Clin. 24 (1) (2006) 35–51, https://doi.org/10.1016/j.det.2005.09.006.
[11] J.A. Ruszkiewicz, A. Pinkas, B. Ferrer, T.V. Peres, A. Tsatsakis, M. Aschner, Neurotoxic effect of active ingredients in sunscreen products, a contemporary review, Toxicol. Reports. 4 (2017) 245–259, https://doi.org/10.1016/j.toxrep.2017.05.006.
[12] R. Alvarez-Román, Biodegradable polymer nanocapsules containing a sunscreen agent: preparation and photoprotection, Eur. J. Pharm. Biopharm. 52 (2001) 191–195, https://doi.org/10.1016/S0939-6411(01)00188-6.
[13] Laure Brinon, Sandrine Geiger, Valérie Alard, Jean Doucet, Jean-François Tranchant, Guy Couarraze, Percutaneous absorption of sunscreens from liquid crystalline phases, J. Control. Release. 60 (1) (1999) 67–76, https://doi.org/10.1016/S0168-3659(99)00054-1.
[14] P. Perugini, S. Simeoni, S. Scalia, I. Genta, T. Modena, B. Conti, F. Pavanetto, Effect of nanoparticle encapsulation on the photostability of the sunscreen agent, 2-ethylhexyl-p-methoxycinnamate, Int. J. Pharm. 246 (1-2) (2002) 37–45, https://doi.org/10.1016/S0378-5173(02)00356-3.

[15] H. Rocha e Silva, G.M. da Luz, C.Y. Satake, B.C. Correa, V.H.V. Sarmento, G.H. de Oliveira, F.C. Carvalho, M. Chorilli, M.P.D. Gremião, Surfactant-based Transdermal System for Fluconazole Skin Delivery, J. Nanomed. Nanotechnol. 05 (2014), https://doi.org/10.4172/2157-7439.1000231.
[16] RyanF Donnelly, Rahamatullah Shaikh, ThakurRaghu Raj Singh, MartinJames Garland, ADavid Woolfson, Mucoadhesive drug delivery systems, J. Pharm. Bioallied Sci. 3 (1) (2011) 89, https://doi.org/10.4103/0975-7406.76478.
[17] G.A.D.S. Cintra, L.A. Pinto, G.M.F. Calixto, C.P. Soares, E.D.S. Von Zuben, M.V. Scarpa, M. Palmira, M.P. Gremião, M. Chorilli, Bioadhesive Surfactant Systems for Methotrexate Skin Delivery, Molecules. 21 (2016) 1–13, https://doi.org/10.3390/molecules21020231.
[18] Chenyu Guo, Jun Wang, Fengliang Cao, Robert J. Lee, Guangxi Zhai, Lyotropic liquid crystal systems in drug delivery, Drug Discov. Today. 15 (23-24) (2010) 1032–1040, https://doi.org/10.1016/j.drudis.2010.09.006.
[19] Ambreen Shoaib, Bharti Mangla, Shamama Javed, Muhammad H. Sultan, Saad S. Alqahtani, Faiyaz Shakeel, Vicissitudes of liquid crystals for solubility enhancement of poorly soluble drugs, J. Mol. Liq. 321 (2021) 114924, https://doi.org/10.1016/j.molliq.2020.114924.
[20] Francesca Damiani Victorelli, Giovana Maria Fioramonti Calixto, Karen Cristina dos Santos, Hilde Harb Buzzá, Marlus Chorilli, Curcumin-loaded Polyethyleneimine and chitosan polymer-based Mucoadhesive liquid crystalline systems as a potential platform in the treatment of cervical Cancer, J. Mol. Liq. 325 (2021) 115080, https://doi.org/10.1016/j.molliq.2020.115080.
[21] J. Bernegossi, G. Calixto, P. Sanches, C. Fontana, E. Cilli, S. Garrido, M. Chorilli, Peptide KSL-W-Loaded Mucoadhesive Liquid Crystalline Vehicle as an Alternative Treatment for Multispecies Oral Biofilm, Molecules. 21 (2015) 37, https://doi.org/10.3390/molecules21010037.
[22] Giovana Maria Fioramonti Calixto, Francesca Damiani Victorelli, Michelle Franz-Montan, Fátima Baltazar, Marlus Chorilli, Innovative mucoadhesive precursor of liquid crystalline system loading anti-gellatinolytic peptide for topical treatment of oral cancer, J. Biomed. Nanotechnol. 17 (2) (2021) 253–262, https://doi.org/10.1166/jbn.2021.3025.
[23] Matheus Aparecido dos Santos Ramos, Giovana Maria Fioramonti Calixto, Luciani Gaspar de Toledo, Bruna Vidal Bonifácio, Lourdes Campaner dos Santos, Margarete Teresa Gottardo de Almeida, Marlus Chorilli, Taís Maria Bauab, Liquid crystal precursor mucoadhesive system as a strategy to improve the prophylactic action of Syngonanthus nitens (Bong.) Ruhland against infection by Candida krusei, Int. J. Nanomedicine (2015) 7455, https://doi.org/10.2147/IJN10.2147/IJN.S92638.
[24] C.C. Müller-Goymann, Physicochemical characterization of colloidal drug delivery systems such as reverse micelles, vesicles, liquid crystals and nanoparticles for topical administration, Eur. J. Pharm. Biopharm. 58 (2) (2004) 343–356, https://doi.org/10.1016/j.ejpb.2004.03.028.
[25] Jan P.F. Lagerwall, Giusy Scalia, A new era for liquid crystal research: Applications of liquid crystals in soft matter nano-, bio- and microtechnology, Curr. Appl. Phys. 12 (6) (2012) 1387–1412, https://doi.org/10.1016/j.cap.2012.03.019.
[26] M. Chorilli, P.S. Prestes, R.B. Rigon, G.R. Leonardi, L.A. Chiavacci, M.V. Scarpa, Desenvolvimento de sistemas líquido-cristalinos empregando silicone fluido de co-polímero glicol e poliéter funcional siloxano, Quim. Nova. 32 (2009) 1036–1040, https://doi.org/10.1590/S0100-40422009000400035.
[27] Andressa T. Fujimura, Renata M. Martinez, Felipe A. Pinho-Ribeiro, Amélia M. Lopes Dias da Silva, Marcela M. Baracat, Sandra R. Georgetti, Waldiceu A. Verri, Marlus Chorilli, Rubia Casagrande, Resveratrol-Loaded Liquid-Crystalline System Inhibits UVB-Induced Skin Inflammation and Oxidative Stress in Mice, J. Nat. Prod. 79 (5) (2016) 1329–1338, https://doi.org/10.1021/acs.jnatprod.5b01132.
[28] N. Gabboun, Release of salicylic acid, diclofenac acid and diclofenac acid salts from isotropic and anisotropic nonionic surfactant systems across rat skin, Int. J. Pharm. 212 (2001) 73–80, https://doi.org/10.1016/S0378-5173(00)00585-8.
[29] Vamshi Krishna Rapalli, Tejashree Waghule, Neha Hans, Arisha Mahmood, Srividya Gorantla, Sunil Kumar Dubey, Gautam Singhvi, Insights of lyotropic liquid crystals in topical drug delivery for targeting various skin disorders, J. Mol. Liq. 315 (2020) 113771, https://doi.org/10.1016/j.molliq.2020.113771.
[30] Paula Souza Prestes, Marlus Chorilli, Leila Aparecida Chiavacci, Maria Virgínia Scarpa, Gislaine Ricci Leonardi, Physicochemical Characterization and Rheological Behavior Evaluation of the Liquid Crystalline Mesophases Developed with Different Silicones, J. Dispers. Sci. Technol. 31 (1) (2009) 117–123, https://doi.org/10.1080/01932690903123841.
[31] B. Fonseca-Santos, C.Y. Satake, G.M.F. Calixto, A.M. Dos Ssantos, M. Chorilli, Trans-resveratrol-loaded nonionic lamellar liquid-crystalline systems: Structural, rheological, mechanical, textural, and bioadhesive characterization and evaluation of in vivo anti-inflammatory activity, Int. J. Nanomedicine. (2017), https://doi.org/10.2147/IJN.S138629.
[32] B. Fonseca-Santos, A.M. dos Santos, C.F. Rodero, M.P. Daflon Gremião, M. Chorilli, Design, characterization, and biological evaluation of curcumin-loaded surfactant-based systems for topical drug delivery, Int. J. Nanomedicine. 11 (2016) 4553–4562, https://doi.org/10.2147/ijn.s108675.
[33] Francesca Damiani Victorelli, Giovana Maria Fioramonti Calixto, Matheus Aparecido Dos Santos Ramos, Taís Maria Bauab, Marlus Chorilli, Metronidazole-Loaded Polyethyleneimine and Chitosan-Based Liquid Crystalline System for Treatment of Staphylococcal Skin Infections, J. Biomed. Nanotechnol. 14 (1) (2018) 227–237, https://doi.org/10.1166/jbn.2018.2484.
[34] A.H. Prado, M.C. Borges, J.O. Eloy, R.G. Peccinini, M. Chorilli, An ultra-high performance liquid chromatography method to determine the skin penetration of an octyl methoxycinnamate-loaded liquid crystalline system, Pharmazie. 72 (2017) 563–567, https://doi.org/10.1691/ph.2017.7037.
[35] Elka Touitou, Victor M Meidan, Ehud Horwitz, Methods for quantitative determination of drug localized in the skin, J. Control. Release. 56 (1-3) (1998) 7–21, https://doi.org/10.1016/S0168-3659(98)00060-1.
[36] Elizângela Abreu Dutra, Daniella Almança Gonçalves da Costa Oliveira, Erika Rosa Maria Kedor-Hackmann, Maria Inês Rocha Miritello Santoro, Determination of sun protection factor (SPF) of sunscreens by ultraviolet spectrophotometry, Rev. Bras. Ciências Farm. 40 (3) (2004) 381–385, https://doi.org/10.1590/S1516-93322004000300014.
[37] R.D. Mansur, João de Souza; Breder, Mário Nei Rodrigues; Mansur, Maria Cristina d'Ascenção; Azulay, Determinação do fator de proteção solar por espectrofotometria, An. Bras. Dermatol. 61 (1986) 121–124.
[38] Robert M. Sayre, Patricia Poh Agin, Gordon J. LeVee, Edward Marlowe, A COMPARISON OF IN VIVO AND IN VITRO TESTING OF SUNSCREENING FORMULAS, Photochem. Photobiol. 29 (3) (1979) 559–566, https://doi.org/10.1111/php.1979.29.issue-310.1111/j.1751-1097.1979.tb07090.x.
[39] Flávia Chiva Carvalho, Giovana Calixto, Ilka Narita Hatakeyama, Gabriela Marielli Luz, Maria Palmira Daflon Gremião, Marlus Chorilli, Rheological, mechanical, and bioadhesive behavior of hydrogels to optimize skin delivery systems, Drug Dev. Ind. Pharm. 39 (11) (2013) 1750–1757, https://doi.org/10.3109/03639045.2012.734510.
[40] Jonatas L. Duarte, Thais C. Taira, Leonardo Delello Di Filippo, Bruno Fonseca-Santos, Mara Cristina Pinto, Marlus Chorilli, Novel bioadhesive polycarbophil-based liquid crystal systems containing Melaleuca alternifolia oil as potential repellents against Aedes aegypti, J. Mol. Liq. 314 (2020) 113626, https://doi.org/10.1016/j.molliq.2020.113626.
[41] B. Fonseca-Santos, C. Del Nero Pacheco, M.C. Pinto, M. Chorilli, An effective mosquito-repellent topical product from liquid crystal-based tea tree oil, Ind. Crops Prod. 128 (2019) 488–495, https://doi.org/10.1016/j.indcrop.2018.11.020.
[42] R.A. Khalil, A.A. Zarari, Theoretical estimation of the critical packing parameter of amphiphilic self-assembled aggregates, Appl. Surf. Sci. 318 (2014) 85–89, https://doi.org/10.1016/j.apsusc.2014.01.046.
[43] E. Berbel Manaia, M. Paiva Abuçafy, B.G. Chiari-Andréo, B. Lallo Silva, J.A. Oshiro-Júnior, L. Chiavacci, Physicochemical characterization of drug nanocarriers, Int. J. Nanomedicine. 12 (2017) 4991–5011, https://doi.org/10.2147/IJN.S133832.
[44] N.C. Rissi, D.A.S. Guglielmi, M.A. Corrêa, L.A. Chiavacci, Relationship between composition and organizational levels of nanostructured systems formed by Oleth 10 and PPG-5-Ceteth-20 for potential drug delivery, Brazilian J. Pharm. Sci. 50 (2014) 653–661, https://doi.org/10.1590/S1984-82502014000300025.
[45] Zhaolu Zhu, Yinglei Zhai, Ning Zhang, Donglei Leng, Pingtian Ding, The development of polycarbophil as a bioadhesive material in pharmacy, Asian J. Pharm. Sci. 8 (4) (2013) 218–227, https://doi.org/10.1016/j.ajps.2013.09.003.
[46] Mutaz B. Habal, The Biologic Basis for the Clinical Application of the Silicones, Arch. Surg. 119 (7) (1984) 843, https://doi.org/10.1001/archsurg.1984.01390190081019.
[47] Yiming Huang, Shuangying Gui, Factors affecting the structure of lyotropic liquid crystals and the correlation between structure and drug diffusion, RSC Adv. 8 (13) (2018) 6978–6987, https://doi.org/10.1039/C7RA12008G.
[48] M.C.C. Urban, D.S. Landgraf, M.H. Oyafuso, L.A. Chiavacci, V.H.V. Sarmento, M. Chorilli, M.A. Corrêa, M.P.D. Gremião, Development and In Vitro Skin Delivery of Dexamethasone Acetate-Loaded Surfactant-Based Systems, J. Nanopharmaceutics Drug Deliv. 1 (2013) 323–334, https://doi.org/10.1166/jnd.2013.1024.
[49] Matthew L. Lynch, Akua Ofori-Boateng, Amanda Hippe, Kelly Kochvar, Patrick T. Spicer, Enhanced loading of water-soluble actives into bicontinuous cubic phase liquid crystals using cationic surfactants, J. Colloid Interface Sci. 260 (2) (2003) 404–413, https://doi.org/10.1016/S0021-9797(02)00016-4.
[50] Britta Siekmann, Heike Bunjes, Michel H.J. Koch, Kirsten Westesen, Preparation and structural investigations of colloidal dispersions prepared from cubic monoglyceride–water phases, Int. J. Pharm. 244 (1-2) (2002) 33–43, https://doi.org/10.1016/S0378-5173(02)00298-3.
[51] Lise Sylvest Nielsen, Lise Sylvest Helledi, Lene Schubert, Release Kinetics of Acyclovir from a Suspension of Acyclovir Incorporated in a Cubic Phase Delivery System, Drug Dev. Ind. Pharm. 27 (10) (2001) 1073–1081, https://doi.org/10.1081/DDC-100108370.
[52] M.J. Fresno, A. Ramírez, M. Jiménez, Systematic study of the flow behaviour and mechanical properties of Carbopol® Ultrez™ 10 hydroalcoholic gels, Eur. J. Pharm. Biopharm. 54 (2002) 329–335, https://doi.org/10.1016/S0939-6411(02)00080-2.
[53] Matthieu Pouzot, Raffaele Mezzenga, Martin Leser, Laurent Sagalowicz, Samuel Guillot, Otto Glatter, Structural and Rheological Investigation of Fd 3 m Inverse Micellar Cubic Phases, Langmuir. 23 (19) (2007) 9618–9628, https://doi.org/10.1021/la701206a.
[54] Carlos Rodríguez-Abreu, Miguel García-Roman, Hironobu Kunieda, Rheology and Dynamics of Micellar Cubic Phases and Related Emulsions, Langmuir. 20 (13) (2004) 5235–5240, https://doi.org/10.1021/la0498962.
[55] Giovana Maria Fioramonti Calixto, Francesca Damiani Victorelli, Lívia Nordi Dovigo, Marlus Chorilli, Polyethyleneimine and Chitosan Polymer-Based Mucoadhesive Liquid Crystalline Systems Intended for Buccal Drug Delivery, AAPS PharmSciTech. 19 (2) (2018) 820–836, https://doi.org/10.1208/s12249-017-0890-2.

[56] D.S. Jones, A.D. Woolfson, J. Djokic, Texture profile analysis of bioadhesive polymeric semisolids: Mechanical characterization and investigation of interactions between formulation components, J. Appl. Polym. Sci. 61 (1996) 2229–2234, https://doi.org/10.1002/(sici)1097-4628(19960919)61:12<2229::aid-app24>3.3.co;2-8.
[58] John Woodley, Bioadhesion, Clin. Pharmacokinet. 40 (2) (2001) 77–84, https://doi.org/10.2165/00003088-200140020-00001.
[59] N. Leveque, S. Makki, J. Hadgraft, Ph. Humbert, Comparison of Franz cells and microdialysis for assessing salicylic acid penetration through human skin, Int. J. Pharm. 269 (2) (2004) 323–328, https://doi.org/10.1016/j.ijpharm.2003.09.012.
[60] Y. Chen, P. Ma, S. Gui, Cubic and Hexagonal Liquid Crystals as Drug Delivery Systems, Biomed Res. Int. 2014 (2014) 1–12, https://doi.org/10.1155/2014/815981.
[61] David Potter, Ewan D. Booth, Henk C.A. Brandt, Robert W. Loose, Robert A.J. Priston, Alan S. Wright, William P. Watson, Studies on the dermal and systemic bioavailability of polycyclic aromatic compounds in high viscosity oil products, Arch. Toxicol. 73 (3) (1999) 129–140, https://doi.org/10.1007/s002040050597.
[62] Chia-Jung TSAI, Li-Ren HSU, Jia-You FANG, Hung-Hong LIN, Chitosan Hydrogel as a Base for Transdermal Delivery of Berberine and Its Evaluation in Rat Skin, Biol. Pharm. Bull. 22 (4) (1999) 397–401, https://doi.org/10.1248/bpb.22.397.
[63] Athanasia Varvaresou, Percutaneous absorption of organic sunscreens, J. Cosmet. Dermatol. 5 (1) (2006) 53–57, https://doi.org/10.1111/jcd.2006.5.issue-110.1111/j.1473-2165.2006.00223.x.
[64] M.S. de S. de B. Monteiro, R.A. Ozzetti, A.L. Vergnanini, L. de Brito-Gitirana, N. M. Volpato, Z.M.F. de Freitas, E. Ricci-Júnior, E.P. dos Santos, Evaluation of octyl p-methoxycinnamate included in liposomes and cyclodextrins in anti-solar preparations: preparations, characterizations and in vitro penetration studies, Int. J. Nanomedicine. (2012) 3045. doi:10.2147/IJN.S28550.
[65] M. Vettor, S. Bourgeois, H. Fessi, J. Pelletier, P. Perugini, F. Pavanetto, M.A. Bolzinger, Skin absorption studies of octyl-methoxycinnamate loaded poly(D, L-lactide) nanoparticles: Estimation of the UV filter distribution and release behaviour in skin layers, J. Microencapsul. 27 (3) (2010) 253–262, https://doi.org/10.3109/10717540903097770.
[66] S. Scalia, M. Mezzena, D. Ramaccini, Encapsulation of the UV Filters Ethylhexyl Methoxycinnamate and Butyl Methoxydibenzoylmethane in Lipid Microparticles: Effect on in vivo Human Skin Permeation, Skin Pharmacol. Physiol. 24 (4) (2011) 182–189, https://doi.org/10.1159/000324054.
[67] Murali K. Matta, Jeffry Florian, Robbert Zusterzeel, Nageswara R. Pilli, Vikram Patel, Donna A. Volpe, Yang Yang, Luke Oh, Edward Bashaw, Issam Zineh, Carlos Sanabria, Sarah Kemp, Anthony Godfrey, Steven Adah, Sergio Coelho, Jian Wang, Lesley-Anne Furlong, Charles Ganley, Theresa Michele, David G. Strauss, Effect of Sunscreen Application on Plasma Concentration of Sunscreen Active Ingredients, JAMA. 323 (3) (2020) 256, https://doi.org/10.1001/jama.2019.20747.
[68] Alice Haddad do Prado, Victor Hugo Sousa Araújo, Josimar O. Eloy, Bruno Fonseca-Santos, Marcelo A. Pereira-da-Silva, Rosângela Gonçalves Peccinini, Marlus Chorilli, Synthesis and Characterization of Nanostructured Lipid Nanocarriers for Enhanced Sun Protection Factor of Octyl p-methoxycinnamate, AAPS PharmSciTech. 21 (4) (2020), https://doi.org/10.1208/s12249-019-1547-0.
[69] Eduardo Ricci-Junior, Gisela Maria Dellamora Ortiz, Elisabete Pereira dos Santos, Aline de Carvalho Varjão Mota, Rafael Antonio Ozzetti, André Luiz Vergnanini, Ralph Santos-Oliveira, Ronald Santos Silva, Vanessa Lira Ribeiro, Zaida Maria Faria de Freitas, In vivo and in vitro evaluation of octyl methoxycinnamate liposomes, Int. J. Nanomedicine (2013) 4689, https://doi.org/10.2147/IJN10.2147/IJN.S51383.